doi:10.1093/brain/awy028 BRAIN 2018: 0; 1–11 | 1

BRAIN
A JOURNAL OF NEUROLOGY

Optical coherence tomography in autosomal recessive spastic ataxia of Charlevoix-Saguenay

Michael H. Parkinson,[1,2] Ana P. Bartmann,[2] Lisa M. S. Clayton,[2] Suran Nethisinghe,[1] Rolph Pfundt,[3] J. Paul Chapple,[4] Mary M. Reilly,[1,2,5] Hadi Manji,[2] Nicholas J. Wood,[1,2] Fion Bremner[2] and Paola Giunti[1,2]

Autosomal recessive spastic ataxia of Charlevoix-Saguenay is a rare neurodegenerative disorder caused by mutations in the *SACS* gene. Thickened retinal nerve fibres visible on fundoscopy have previously been described in these patients; however, thickening of the retinal nerve fibre layer as demonstrated by optical coherence tomography appears to be a more sensitive and specific feature. To test this observation, we assessed 292 individuals (191 patients with ataxia and 101 control subjects) by peripapillary time-domain optical coherence tomography. The patients included 146 with a genetic diagnosis of ataxia (17 autosomal spastic ataxia of Charlevoix-Saguenay, 59 Friedreich's ataxia, 53 spinocerebellar ataxias, 17 other genetically confirmed ataxias) and 45 with cerebellar ataxia of unknown cause. The controls included 13 asymptomatic heterozygotes for *SACS* mutations and 88 unaffected controls. The cases with autosomal recessive spastic ataxia of Charlevoix-Saguenay included 11 previously unpublished *SACS* mutations, of which seven were nonsense and four missense mutations. Most patients were visually asymptomatic and had no previous history of ophthalmic complaints and normal or near normal visual test results. None had visual symptoms directly attributable to the retinal changes. Twelve of the 17 cases (70.6%) had thickened retinal nerve fibres visible on fundoscopy. All patients with autosomal recessive spastic ataxia of Charlevoix-Saguenay had thickening of the peripapillary retinal nerve fibre layer on optical coherence tomography, whereas all the remaining cases and controls except one showed normal or reduced average peripapillary retinal nerve fibre layer thickness on optical coherence tomography. We propose a cut-off value of 119 μm in average peripapillary retinal nerve fibre layer thickness, which provides a sensitivity of 100% and specificity of 99.4% amongst patients affected with ataxia. This is the largest cohort of patients with this condition to undergo systematic evaluation by optical coherence tomography. This is a useful tool in identifying cases of autosomal recessive spastic ataxia of Charlevoix-Saguenay from other causes of ataxia. Visualization of thickened retinal fibres by direct fundoscopy is less sensitive. We therefore advocate the use of this technique in the assessment of possible cases of this condition.

1 Department of Molecular Neuroscience, UCL Institute of Neurology, London, UK
2 National Hospital for Neurology and Neurosurgery, Queen Square, London, UK
3 Department of Human Genetics, Radboud University, Nijmegen Medical Centre, Nijmegen, The Netherlands
4 William Harvey Research Institute, Barts and The London School of Medicine and Dentistry, Queen Mary University of London, UK
5 MRC Centre for Neuromuscular Diseases, UCL Institute of Neurology, London, UK

Correspondence to: Prof Paola Giunti
Department of Molecular Neuroscience, UCL Institute of Neurology, Queen Square House, Queen Square, London, WC1N 3BG, UK
E-mail: p.giunti@ucl.ac.uk

Correspondence may also be addressed to: Dr Fion Bremner
Department of Neuro-ophthalmology, National Hospital for Neurology and Neurosurgery, Queen Square, London, WC1N 3BG, UK
E-mail: f.bremner@nhs.net

Received May 26, 2017. Revised December 13, 2017. Accepted December 18, 2017

Keywords: autosomal recessive spastic ataxia of Charlevoix-Saguenay; optical coherence tomography; retinal nerve fibre layer; ataxia

Abbreviations: ARSACS = autosomal recessive spastic ataxia of Charlevoix-Saguenay; FRDA = Friedreich's ataxia; OCT = optical coherence tomography; RNFL = retinal nerve fibre layer; SCA = spinocerebellar ataxia

Introduction

Autosomal recessive spastic ataxia of Charlevoix-Saguenay (ARSACS; OMIM 270550) is a rare neurodegenerative disorder characterized by a slowly progressive cerebellar ataxia, spasticity and demyelinating peripheral neuropathy, causing incoordination, dysarthria, cerebellar eye signs, limb weakness, muscle cramps, distal amyotrophy, sensory loss, pyramidal signs and skeletal foot abnormalities. The condition was first described in the late 1970s among founder populations in the Charlevoix and Saguenay-Lac-St-Jean regions of North-Eastern Québec, but cases have subsequently been identified around the world. The causative gene on chromosome 13q12.12 is named *SACS* and was identified by Engert *et al.* (2000) with an open reading frame of 13 737 base pairs (Ouyang *et al.*, 2006). More than 100 different mutations have now been described (Thiffault *et al.*, 2013).

The large number of mutations meant that diagnostic testing previously required Sanger sequencing of the entire gene. Custom panel next generation sequencing techniques are transforming this field and are becoming less expensive and more available year by year. However, they are still not available in many centres. Given the large quantity of genetic information produced by these techniques, it is more important than ever to have clinical tests that guide focused genetic testing. In addition, new genetic variants from next generation sequencing techniques can be challenging to interpret regarding pathogenicity. Further deep phenotyping, including supportive clinical tests, is vital whilst awaiting reliable functional studies to interpret new genetic variants. In the field of ARSACS, optical coherence tomography (OCT) may be an important supportive clinical test.

OCT is used by ophthalmologists to investigate retinal disease and optic neuropathy. Thinning of the peripapillary retinal nerve fibre layer (RNFL) is seen in glaucoma, optic nerve inflammation, ischaemia and compression, as well as in multiple sclerosis, Alzheimer's disease, Parkinson's disease, hereditary spastic paraparesis type 7 (SPG7), epilepsy and with various drugs such as vigabatrin (Jindahra *et al.*, 2010; Clayton *et al.*, 2011; Klebe *et al.*, 2012; Balestrini *et al.*, 2016). RNFL thinning has been demonstrated in the cerebellar subtype of multiple system atrophy (MSA-C) and spinocerebellar ataxia (SCA) types 1–3, 6 and 7 (Manrique *et al.*, 2009; Pula *et al.*, 2011). In Friedreich's ataxia (FRDA), RNFL thinning correlates both with markers of clinical severity and the underlying genetic process (Fortuna *et al.*, 2009; Noval *et al.*, 2012; Seyer *et al.*, 2013). Thus, thinning of the peripapillary RNFL seems to be a common feature of neurodegenerative disease, even in patients with little or no evidence of visual dysfunction.

By contrast, thickening of the RNFL is generally only seen in conditions causing a swollen optic disc, such as the acute stage of inflammatory or ischaemic optic neuropathy, Leber's hereditary optic neuropathy, papilloedema or central retinal vein occlusion (Barboni *et al.*, 2005; Karam and Hedges, 2005; Savini *et al.*, 2006). Patients with retinitis pigmentosa also have RNFL thickening (Hood *et al.*, 2009), although in these cases there is gross disruption to the outer retinal layers making interpretation of these RNFL measurements unclear. RNFL thickening is therefore not normally seen in the context of chronic progressive neurodegenerative disease. ARSACS may be an exception to this rule.

The earliest clinical descriptions of ARSACS recorded 'striking and markedly increased visibility of the retinal nerve fibers, mainly in the papillomacular bundle area' (Bouchard *et al.*, 1978). However, these fundoscopic appearances have been inconsistently observed in non-Québecois cases (Mrissa *et al.*, 2000; Gücüyener *et al.*, 2001; Grieco *et al.*, 2004; Takiyama, 2006; Vermeer *et al.*, 2008; Garcia-Martin *et al.*, 2013). OCT scans in ARSACS have confirmed abnormal thickening of the RNFL (Desserre *et al.*, 2011; Nethisinghe *et al.*, 2011; Pablo *et al.*, 2011; Vingolo *et al.*, 2011; Gazulla *et al.*, 2012; Garcia-Martin *et al.*, 2013; Stevens *et al.*, 2013) although one series reported a single case with peripapillary RNFL thicknesses of 86 and 111 µm, which were within the range for unaffected controls (Yu-Wai-Man *et al.*, 2014). Furthermore, in a previous study we reported that two unaffected individuals in a single family who were heterozygous for two different *SACS* mutations showed partial peripapillary RNFL thickening with a mean of thickness of 115.5 µm (Nethisinghe *et al.*, 2011). This finding has recently been confirmed in five heterozygotes for two different mutations, which showed average peripapillary RNFL thickness of between 104 and 132 µm (Van Lint *et al.*, 2016).

It is therefore not clear whether RNFL thickening as detected by OCT is present in all cases of ARSACS, nor is it known whether similar OCT changes may be seen in patients with other non-ARSACS causes of ataxia or heterozygous carriers of *SACS* mutations (Parkinson *et al.*, 2014). To address these questions, we measured RNFL thickness by OCT in ataxia patients who were referred to our tertiary hospital specialist ataxia centre and compared them with a large cohort of controls that included first degree relatives of known patients with ARSACS.

Subjects and methods

Study population and genetic analysis

Patients were recruited from the Ataxia Centre of the National Hospital for Neurology and Neurosurgery (NHNN) in London UK, which receives referrals for specialist opinions from across the UK and internationally. The majority of patients live in London and the Southeast of England and are of UK descent. All patients gave informed consent, and the study was given approval by the London Brent Research Ethics Committee (reference 12/LO/1291) and complied with the Declaration of Helsinki. In total, 292 individuals were assessed including 191 patients with ataxia and 101 controls. The 101 controls included 88 unaffected individuals and 13 unaffected first-degree relatives of patients subsequently diagnosed in the study with ARSACS (and subsequently confirmed as heterozygotes for *SACS* gene mutations).

At the commencement of the study, of the 191 patients with ataxia, 59 had a genetic diagnosis of FRDA and 53 had various SCAs. The remaining 79 did not have a genetic diagnosis. All 191 had OCT scans and those that showed RNFL thickening (as defined as average peripapillary RNFL thickness above the 95th centile of the scanner's normative data) underwent genetic analysis in the Department of Human Genetics, Radboud University, Nijmegen Medical Centre, Nijmegen, Netherlands, using previously described methods (Vermeer *et al.*, 2008). DNA was extracted from peripheral blood lymphocytes using standard procedures. All cases were extensively investigated with biochemical, metabolic, genetic and other tests showing no evidence of an alternative diagnosis (Supplementary Table 2). This revealed the 17 cases of ARSACS discussed in the study. *SACS* gene variants were annotated according to reference sequence NM_014363.

The remainder continued to undergo routine genetic testing in our institution, which revealed 13 cases of various genetically determined ataxias: ataxia with oculomotor apraxia type 2 (AOA2), episodic ataxia types 1 and 2 (EA1/2), fragile X tremor ataxia syndrome (FXTAS), ataxia with fibroblast growth factor mutation (FGF), Sjögren-Larsson syndrome (SLS) and ataxia with co-enzyme Q_{10} deficiency ($ACoQ_{10}D$). The patient with $ACoQ_{10}D$ had a pathogenic mutation in the aarF domain-containing kinase 3 gene (now known as *COQ8A*).

The remaining 49 cases with no genetic diagnosis were subjected to an Illumina TruSeq Custom Amplicon panel (Illumina) covering 10 genes known to cause spastic ataxia (Supplementary Table 1). Library preparation was undertaken using the manufacturer's protocol (part 15027983, revision C, August 2013) using MiSeq reagent kit version 3 with amplicons designed to cover *SACS* gene exons with 99% coverage. Subsequent amplification used the polymerase chain reaction (PCR) according to the manufacturer's protocol (Applied Biosystems Gene Amp PCR System 9700, Thermo Fisher Scientific) and massively parallel sequencing used the MiSeq sequencer (Illumina). This technique revealed four cases of SPG7. The 13 heterozygous *SACS* gene carriers were also diagnosed using this technique. This left 45 cases of cerebellar ataxia of unknown cause. These patients had previously been assessed routinely in the NHNN Ataxia Centre and undergone extensive clinically appropriate genetic, metabolic and other diagnostic tests (Supplementary Table 1). The demographic details and diagnoses of all patients are given in Table 1.

Optical coherence tomography

After dilating the pupils with 1% tropicamide eye drops, the patients were seated at a time-domain OCT (TD-OCT) device (Stratus, Carl Zeiss Meditec) and asked to fixate on the device's internal target using the test eye while the fellow eye was occluded. Polarization was machine-optimized then the RNFL thickness was measured in a circle around the optic disc using the 'Fast RNFL Thickness' acquisition protocol. OCT data were analysed using the proprietary software (Stratus version 4.07), which provides automated estimates of RNFL thickness in each quadrant around the disc (superior, nasal, inferior and temporal) and an average measurement of RNFL thickness around the entire circumference of the optic disc. The analysis software also provides a measure of scan quality referred to as 'signal strength' on an arbitrary scale 0–10; we took the decision to accept recordings only if the signal strength was at least 5, the scan circle was well-centred on the optic disc and there was no blink artefact. In each patient, OCT scans were repeated three times per eye, and the results for both eyes averaged. In a small number of cases, imaging of both eyes was not possible for technical reasons such as inability to fixate or poor image quality.

Clinical examination

Each participant with ARSACS underwent full neurological examination by a neurologist experienced in the assessment of patients with ataxia (M.H.P.) using a standard protocol. Age at onset was taken as the age of first symptoms compatible with the subsequent diagnosis of ARSACS as judged by the patient or in the medical notes. Patients had their best corrected visual acuity (Snellen) and colour vision (Ishihara pseudo-isochromatic plates) tested in both eyes, and then underwent a full ophthalmic examination by an experienced ophthalmologist (F.B.) including fundoscopy to determine whether there was clinically apparent abnormal thickening of the RNFL.

Statistical analysis

Statistical analysis was undertaken using IBM SPSS Statistics for Windows, version 21.0 (IBM Corp., Armonk, NY, 2012) and Microsoft Excel (2010). Associations between RNFL thickness and disease duration, age at onset and age at examination were undertaken using linear regression analysis. Differences between RNFL thickness and visual scores between different patient groups were undertaken using analysis of covariance (ANCOVA) with subsequent Mann-Whitney U-tests and Bonferroni correction. Calculations of sensitivity and specificity involved a receiver operating characteristic (ROC).

Results

Patients with ARSACS

The 17 patients with ARSACS came from 11 families (Table 2). The patients were between the ages of 21 and 62 years when assessed. Disease onset varied between 1 and 46 years, and disease duration between 11 and 46

Table 1 Demographic and OCT results by disease group

Group	Participants, *n*	Eyes examined, *n*	Age mean ± SD (range)	M:F ratio	OCT-S Mean ± SD (range)	OCT-N Mean ± SD (range)	OCT-I Mean ± SD (range)	OCT-T Mean ± SD (range)	OCT-Av Mean ± SD (range)
ARSACS	17	34	42.8 ± 13.4 (21–61)	9:8	172.6 ± 19.2 (145.0–200.0)	126.4 ± 18.3 (95.5–152.5)	185.3 ± 21.1 (146.5–225.5)	115.7 ± 21.6 (78.5–153.5)	150.0 ± 16.0 (119.3–174.8)
ARSACS heterozygotes	13	26	47.2 ± 16.9 (25–70)	5:8	115.8 ± 11.2 (94.5–128.5)	78.1 ± 16.4 (54.5–96.5)	120.0 ± 13.4 (92.0–145.5)	61.3 ± 9.1 (50.5–81.5)	93.8 ± 7.5 (82.0–105.5)
FRDA	59	113	31.7 ± 11.7 (15–61)	32:27	88.5 ± 25.2 (34.0–150.5)	59.4 ± 20.2 (29.5–140.5)	91.5 ± 21.5 (39.0–134.5)	59.5 ± 11.9 (30.0–84.5)	74.7 ± 15.1 (35.1–104.2)
SCAs	53	96	55.6 ± 14.1 (24–81)	30:23	103.3 ± 20.4 (40.5–136.5)	63.1 ± 17.3 (22.0–114.0)	106.0 ± 20.1 (45.0–139.0)	63.4 ± 18.2 (34.0–130.0)	83.9 ± 13.0 (40.2–103.5)
SCA1	5	9	42.2 ± 8.5 (30–54)	3:2	105.5 ± 22.7 (76.0–132.5)	68.5 ± 18.7 (41.0–83.5)	100.9 ± 26.3 (57.0–120.0)	57.6 ± 11.4 (40.0–68.0)	83.1 ± 18.5 (57.3-101.0)
SCA2	10	18	48.9 ± 11.9 (28–65)	3:7	95.0 ± 25.2 (40.5–122.5)	60.6 ± 13.7 (40.0–79.0)	104.0 ± 24.8 (45.0–135.0)	56.1 ± 12.2 (36.0–77.0)	78.8 ± 16.8 (40.2-98.0)
SCA3	9	13	52.7 ± 10.4 (35–70)	5:4	95.2 ± 18.6 (73.0–136.0)	52.8 ± 19.5 (22.0–81.5)	98.9 ± 15.5 (77.0–121.0)	77.4 ± 31.6 (41.0–130.0)	81.0 ± 7.8 (67.2–94.0)
SCA6	20	39	64.5 ± 11.3 (43–81)	12:8	108.7 ± 18.1 (74.0–136.5)	67.5 ± 17.9 (31.0–114.0)	113.0 ± 16.4 (71.5–139.0)	65.0 ± 13.7 (50.5–103.5)	88.5 ± 10.7 (65.6-103.5)
SCA7	6	12	45.8 ± 16.3 (24–64)	5:1	102.4 ± 20.4 (68.4–128.5)	63.4 ± 18.2 (40.0–81.0)	94.1 ± 19.4 (62.5–113.0)	53.4 ± 9.9 (34.0–60.5)	78.3 ± 14.6 (51.3–90.8)
SCA14	2	3	71.0 (67–75)	1:1	110.0 (106.0–114.0)	61.5 (56.0–67.0)	129.8 (124.0–136.0)	68.3 (60.0–77.0)	92.0 (90.1–94.0)
SCA28	1	2	65	1:0	131	69	99	60	89.4
Other genetic ataxias	17	32	52.1 ± 16.4 (25–77)	7:10	107.6 ± 20.1 (74.5–143.5)	64.7 ± 22.0 (34.0–108.0)	114.3 ± 21.7 (59.0–144.5)	64.1 ± 16.1 (46.0–106.5)	87.7 ± 14.1 (56.3–106.3)
AOA2	6	12	44.2 ± 17.1 (25–73)	3:3	115.3 ± 22.9 (85.5–143.5)	68.5 ± 21.7 (43.5–100.5)	123.5 ± 12.9 (110.5–144.5)	81.2 ± 14.8 (67.5–106.5)	97.0 ± 8.9 (85.4-106.3)
SPG7	4	8	61.0 ± 13.6 (47–77)	3:1	116.6 ± 14.6 (103.5–129.5)	72.3 ± 18.2 (52.0–94.5)	119.8 ± 4.9 (114.0–124.5)	53.4 ± 7.5 (46.0–63.0)	90.4 ± 8.1 (85.1–102.3)
EA1	2	4	51.5 (35–68)	0:2	103.5 (90.5–116.5)	88.0 (68–108)	119.5 (100.5–138.5)	55.0 (53–57)	91.6 (79.0–104.2)
EA2	1	2	44	0:1	99.0	53.0	139.0	58.0	88.5
FXTAS	1	2	72	1:0	74.5	43.5	100.5	46.0	66.4
FGF	1	2	60	0:1	111.0	51.0	78.0	56.0	73.7
SLS	1	1	33	0:1	76.0	34.0	59.0	56.0	56.3
ACoQ$_{10}$D	1	1	64	0:1	105.0	43.0	109.0	65.0	80.0
Ataxia of unknown cause	45	83	50.3 ± 15.2 (21–82)	16:29	112.2 ± 20.7 (52.0–144.5)	72.4 ± 17.3 (39.0–115.0)	117.5 ± 22.2 (61.0–159.5)	62.9 ± 14.4 (30.0–93.5)	91.5 ± 13.4 (45.5–124.0)
All non-ARSACS (excluding heterozygotes)	174	325	45.8 ± 17.2 (15–82)	85:89	101.0 ± 24.0 (34.0–150.5)	64.4 ± 19.3 (22.0–140.5)	104.9 ± 23.6 (39–159.5)	62.0 ± 15.1 (30.0–130.0)	83.1 ± 15.4 (35.1–124.0)
Controls	88	176	43.9 ± 13.1 (20–74)	35:53	115.9 ± 13.9 (78.0–146.0)	73.7 ± 10.6 (52.0–102.0)	122.8 ± 14.5 (92.0–171.0)	65.2 ± 10.2 (44.0–102.0)	94.3 ± 8.8 (78.0–118.0)

ACoQ$_{10}$D = ataxia with co-enzyme Q$_{10}$ deficiency (*ADCK3*/*COQ8A* mutation); AOA = ataxia with oculomotor apraxia; EA = episodic ataxia; FGF = ataxia with fibroblast growth factor mutation; FXTAS = fragile X tremor ataxia syndrome; OCT-S/N/I/T/Av = OCT-superior/nasal/inferior/temporal/average over all quadrants; SCA = spinocerebellar ataxia; SLS = Sjögren-Larsson syndrome; SPG7 = spastic paraparesis type 7.

years. In contrast to previous descriptions of the Québecois cohort of ARSACS patients (Bouchard *et al.*, 1998), members of one family (Family D) had disease onset in middle life (range 35–51 years). All from this family share three pathogenic mutations, none of which is found in the Québecois population (Thiffault *et al.*, 2013). Two mutations (c.8339T>G and c.12416T>C; NM_014363.4) are known from studies of related carriers to co-segregate. All patients in the study had ataxia and all but one had spasticity (94.1%). Fourteen (82.4%) showed clinical evidence of sensory loss. Twelve (70.6%) had limb weakness. Deep tendon reflexes were absent in 10 patients (58.8%) and hyper-reflexic in six (35.3%), sometimes with mixed absent and increased reflexes in the same patient. Thirteen had extensor plantar reflexes (76.5%). Eleven patients had dysarthria (64.7%) and 15 had skeletal foot abnormalities (88.2%). All patients displayed nystagmus.

The 17 patients had 20 different sequence variants (Table 2) of which nine have been published previously (c.1144G>T, c.4744G>T, c.5151dupA, c.5948C>T, c.6 392delT, c.7255_7259delGAGAA, c.11265_11266delAT, c.11352_11353dupAA, c.12028C>T). Five variants were previously described in the thesis of Dr Sascha Vemeer (c.5820_5821delAC, c.7162_7163delAC, c.9404T>C, c.9 956_9957delAA, c.11675C>G) (Vermeer, 2012) and six variants are novel (c.3149C>A, c.4226_4229delATGA,

Table 2 Neurological, ophthalmological and OCT results for patients with ARSACS

Patient	Family group	SACS mutation*	Age at onset	Age at examination	Disease duration	Neurological features									Ophthalmological features						RNFL thickness by TD-OCT				
						Ataxia	Spasticity	Sensory loss	Weakness	Reflexes	Plantar reactions	Nystagmus	Dysarthria	Foot abnormalities	Pupils	Ocular history	Fundoscopy	Other ophthalmic features	Snellen	Ishihara	Superior	Nasal	Inferior	Temporal	Average
1	A	c.1144G>T c.11352_11353dup	1	30	29	+	+	(+)	(+)	N/–/++	E/E	+	+	+	N	–	RT	D	3	100	200	151.5	195.5	152	174.8
2	B	c.7255_7259del c.9956_9957delAA	5	23	18	+	+	–	–	N	–	+	–	+	N	–	RT	A	3	100	156	120	182.5	120.5	144.9
3	C	c.5820_5821del c.7162_7163del	1	33	32	++	++	++	+	N	E/E	+	+	+	N	–	RT	A	4	92	194.5	111.5	179	153.5	159.4
4	D	c.8339T>G c.11675C>G c.12416T>C	48	60	12	++	+	++	+	N	E/F	+	–	–	N	–	(RT)	A	1	100	161	152.5	190.5	84.5	147.1
5	D	c.8339T>G c.11675C>G c.12416T>C	51	62	11	+	+	++	–	N/–	E/E	+	–	–	N	–	RT	A	3	100	152.5	119.5	181.5	100.5	138.5
6	D	c.8339T>G c.11675C>G c.12416T>C	43	61	18	+	++	+	+	N/++	E/E	+	+	+	N	–	N	A	2	100	150	103	146.5	78.5	119.3
7	D	c.8339T>G c.11675C>G c.12416T>C	35	47	12	+	+	+	–	N/++	E/E	+	–	+	N	CB	N	A	2	100	145	133	164.5	94	134.1
8	D	c.8339T>G c.11675C>G c.12416T>C	46	60	14	+	(+)	+	+	N/–	E/E	+	–	+	N	CB	N	A	4	65	148	114	157	93	128.1
9	E	c.5151dupA c.5948C>T c.6392delT	2	40	38	+	+	++	+++	–	E/E	+	–	+	N	–	N	A	4	100	175.5	103.5	157	120	139.4
10	F	c.9404T>C c.11265_11266delAT	10	45	35	+	++	++	+++	–	–	+	+	+	N	LA	RT	A	4	100	188	148	225.5	121	170.7
11	F	c.9404T>C c.11265_11266delAT	13	39	26	(+)	+	++	+	N/++	E/F	+	+	+	N	LA	N	N	4	100	180	147.5	195	114	158.9
12	G	c.6078del homozygous	2	21	19	+	++	–	–	++	E/E	+	+	+	N	M	RT	K	7	100	190	136.5	215	143.5	171.1
13	H	c.4226_4229del c.9404T>C	32	50	18	+	+	++	+	N/–	–	+	+	+	N	–	RT	A	NR	NR	155	126.5	180	121	145.6
14	I	c.3149C>A c.4744G>T	5	32	27	+	(+)	–	–	N/–/++	E/–	+	++	+	N	–	RT	A	2	100	171.5	113.5	182.5	114	145.3
15	J	c.9404T>C c.12028C>T	23	46	23	(+)	–	+++	+	N/–	F/F	+	+	+	N	–	RT	A	4	100	195	127.5	210.5	129	165.6
16	J	c.9404T>C c.12028C>T	5	51	46	+	(+)	++	+	–	E/E	+	+	+	N	–	RT	A	2	100	177	95.5	196	108.5	144.4
17	K	c.9956_9957delAA c.10115dup	1	31	30	(+)	++	(+)	+	N/–	E/E	+	(+)	+	N	–	RT	A	4	100	196	144.5	191.5	119.5	163.0

NR = not recorded. *Reference sequence NM_014363.4.

Ataxia, spasticity, sensory loss, weakness, nystagmus, dysarthria, dysphagia: – = absent; (+) equivocally present; + = present; ++ strongly present; +++ very strongly present. Reflexes: N = normal; – = absent; ++ = increased. Plantar reflexes: E = extensor; F = flexor; – = mute. Foot abnormalities: PC = pes cavus; TEV = talipes equinovarus; TE = talipes equinus; HT = hammer toes; CT = claw toes. Ocular history: CB = colour blind; LA = left eye amblyopia; M = myopia; – = no past ocular history. Fundoscopic appearance: RT = retinal thickening. Other ophthalmic features: D = diplopia; A = asymptomatic; K = keratoconus; N = symptomatic nystagmus.

c.6078delT, c.8339T>G, c.10115dupC, c.12416T>C). Of these 11, seven are pathogenic nonsense mutations. Four are missense variants involving single base pair substitutions (c.3149C>A, c.8339T>G, c.9404T>C, c.12416T>C) and amino acid changes (p.Ala1050Asp, p.Phe2780Cys, p.Leu3153Ser, p.Leu4139Ser; NP_055178.3). All are in the giant exon 10 of the *SACS* gene where the majority of mutations to date have been described. The lowest Grantham score was 126 so that all amino acid changes were predicted to be radical or moderately radical. All four are predicted to affect highly conserved amino acids. All mutations were predicted to be disease-causing by MutationTaster2 software (http://www.mutationtaster.org/) and probably damaging by the Polymorphism Phenotyping Program 2 (PolyPhen-2; http://genetics.bwh.harvard.edu/pph2/). The variants c.1349C>A and c.12416T>C were absent from the 1000 Genomes Project (1000G), the Exome Sequencing Project (ESP), the Database of Single Nucleotide Polymorphisms (dbSNP) and the Genome Aggregation Database (gnomAD). The variant c.9404T>C is recorded in ESP with a frequency of 0.00008 and in gnomAD with a frequency of 0.00001. The variant c.8339T>G is present in all four databases including four homozygotes recorded in gnomAD suggesting that this variant is probably not pathogenic. Since c.8339T>G always co-segregated with c.12416T>C in five siblings who have a nonsense mutation (c.11675C>G) on the other allele, this clarifies which of the two *cis* variants is pathogenic. Further details of the 20 mutations are given in Supplementary Table 3 and of the *in silico* pathogenicity prediction results for the four novel missense mutations in Supplementary Table 4.

The results of the ophthalmological assessment of patients with ARSACS are given in Table 2. In general, patients had no complaints about their eyes or vision. In a few cases there was a history of previous ophthalmic problems (two patients with amblyopia, two with congenital colour blindness and one with myopia). No patients had visual symptoms ascribable to retinal disease, with 14/17 (82.4%) patients visually asymptomatic, one patient with diplopia, one with symptomatic nystagmus and one with focusing problems caused by keratoconus. All patients except the patient with keratoconus had Snellen acuity of 6/9 or better, and only one patient was unable to identify the Ishihara pseudo-isochromatic plates correctly. In all cases pupillary reactions to light were normal. Apart from the one case with keratoconus, no other ARSACS patient was found to have any abnormality in the anterior segment of the eye on slit lamp biomicroscopy.

Fundoscopy revealed abnormal thickening of the RNFL in 13 of 17 patients (76.5%). A typical example of this characteristic fundal appearance is shown in Fig. 1A: the peripapillary RNFL is thickened in all meridians and the abnormality extends for several disc diameters, obscuring in some places the retinal vessels. None of these cases had any associated swelling or elevation of the optic nerve head, nor were there any abnormalities seen in the overlying vitreous, retinal vessels, outer retina, retinal pigment epithelium or choroid. In 4 of the 17 cases of ARSACS (23.5%), fundoscopy was normal with no clinically

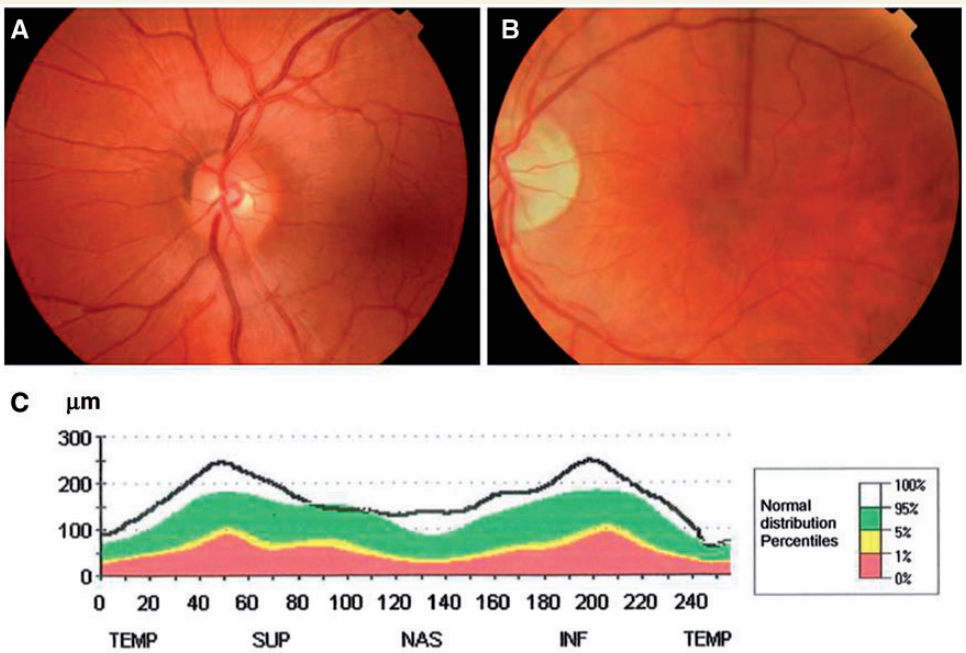

Figure 1 Fundal appearance in ARSACS. (**A**) Peripapillary RNFL thickening apparent on fundal photography for Patient 1 with RNFL of 175 µm on OCT. (**B**) RNFL thickening not apparent on fundal photography for Patient 9 with RNFL of 139 µm on OCT. (**C**) OCT appearance in ARSACS for Patient 15 right eye showing thickening of RNFL (black line). The green band represents the 5th to 95th percentile of the normative data. (Quadrants: TEMP = temporal; SUP = superior; NAS = nasal; INF = inferior).

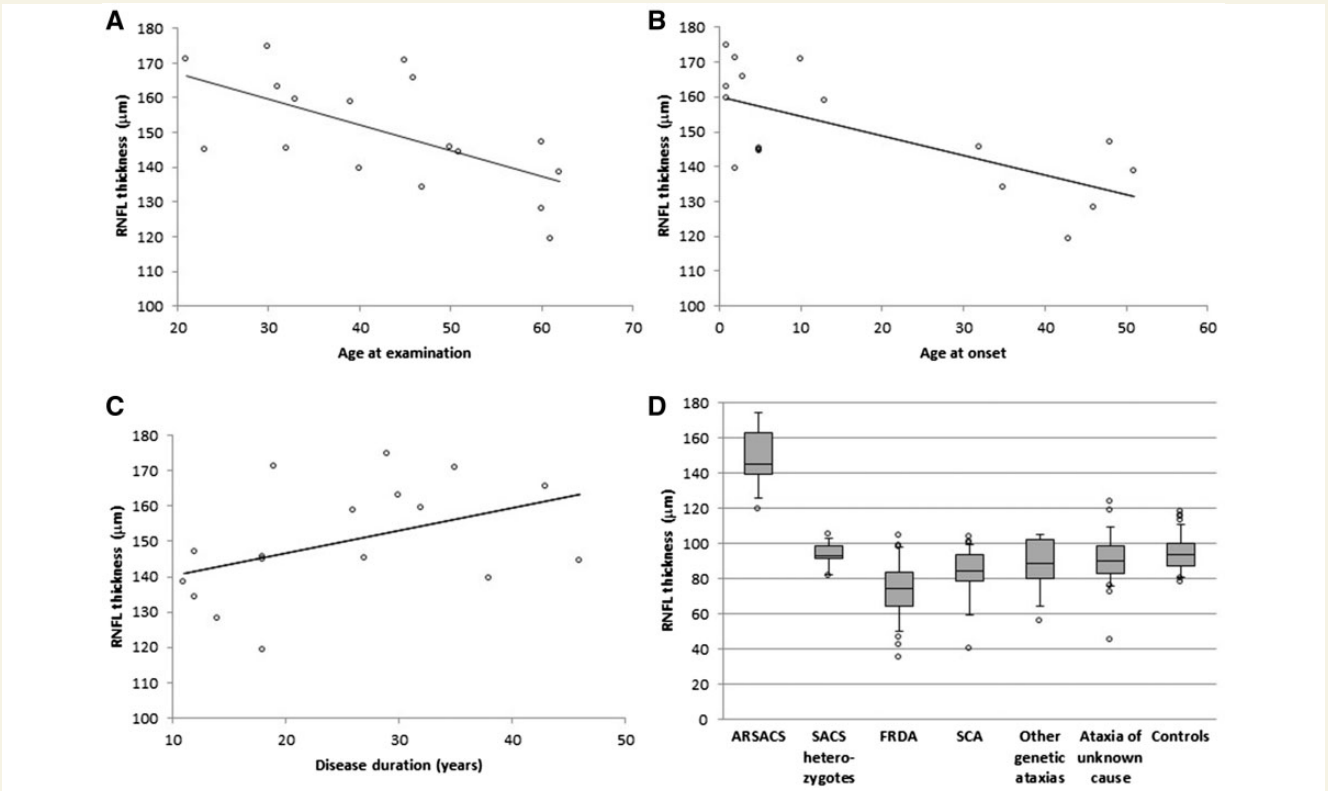

Figure 2 Correlations between average peripapillary RNFL thickness among the ARSACS patients. Correlations between average peripapillary RNFL thickness and (**A**) age at disease onset; (**B**) age at examination; and (**C**) disease duration (n = 17). Linear regression lines shown. (**D**) Box-and-whisker plots of average OCT measurements of peripapillary RNFL thickness in ARSACS, *SACS* gene mutation heterozygotes, FRDA, SCAs, other genetically confirmed ataxias, cerebellar ataxia of unknown cause, and unaffected controls. Boxes show median and interquartile range; whiskers show 5th and 95th percentiles; points show values outside 5th and 95th percentiles.

apparent thickening of the RNFL; an example is shown in Fig. 1B. There was no clear correlation between genotype and retinal phenotype; indeed in Family D, individuals sharing the same mutations had different fundoscopic appearances.

OCT measurements of the peripapillary RNFL thickness in these ARSACS patients are shown in Table 2 (for each patient values shown are the mean of measurements from both eyes unless it was only possible to obtain a scan from one eye). The average peripapillary RNFL thickness measurements (estimated from the entire 360° of the scanned circle around each disc) ranged from 119.3 µm to 174.8 µm, and in all cases lay above the 95% upper limit defined in the normative database provided by the manufacturer. OCT measurements of average peripapillary RNFL thickness were significantly lower in the four cases where fundoscopy was clinically normal [mean = 130.2, standard deviation (SD) = 8.6] than in the remaining 13 cases where it was visibly thickened (mean = 156.1, SD = 12.3; P = 0.001). Further analysis of OCT measurements by quadrant (superior, nasal, inferior and temporal) showed similar degrees of abnormal thickening of the RNFL in all meridians. Among the whole cohort of 17 patients with ARSACS there was a significant decline in average peripapillary RNFL thickness with age (linear regression coefficient R = 0.624, P = 0.007) and a negative correlation with age at onset (linear regression coefficient R = 0.629, P = 0.007) but a non-significant positive correlation with disease duration (linear regression coefficient R = 0.368, P = 0.146; Fig. 2A–C).

Average OCT measurements of the peripapillary RNFL thickness for ARSACS and all other groups studied are shown in Table 1 and displayed as box-and-whisker plots in Fig. 2D. A typical example of an OCT scan in an ARSACS patient is given in Fig. 1C.

SACS gene mutation heterozygotes

Thirteen individuals carrying heterozygous *SACS* gene mutations who were all first-degree relatives of the patients studied had RNFL thickness measured by OCT. Twelve had visual acuity measured, of which two readings were <6/9. Eight had colour vision measured of which all were normal or near-normal. Mean RNFL thickness was 93.8 µm with a range of 82.0 to 105.5 µm.

Patients with other types of genetic ataxia

One hundred and twenty-nine patients with genetically confirmed ataxias other than ARSACS were seen (FRDA, $n = 59$; SCA, $n = 53$; others, $n = 17$). Many but not all of these patients had average peripapillary RNFL thickness measurements below the 95% lower limit of normal compared to the machine's age-matched bank of normative data. None of these patients had average peripapillary RNFL measurements $>107\,\mu m$ whereas all the ARSACS patients had RNFL measurements $>119\,\mu m$, providing an absolute differentiation between cases of ARSACS and other genetically proven ataxias. However, it is important to calculate average peripapillary RNFL thickness, as individual sectoral values may have greater and overlapping ranges (e.g. for the temporal quadrant, the lowest ARSACS value is 78.5 µm, whereas the highest non-ARSACS value is 150.5 µm for a patient with SCA3). There were no significant differences in gender between the seven groups (Pearson χ^2 value 7.939 with 6 degrees of freedom, $P = 0.243$) but there were significant differences in age between the groups (ANOVA $P < 0.0005$). In particular, the mean age of patients with FRDA was significantly less than all other groups except the ARSACS patients. The only significant difference in age between the ARSACS group and any other group was with the SCA group ($P = 0.02$, Mann-Whitney U-test with Bonferroni correction). Using an ANCOVA corrected for age (covariates evaluated at 45.1 years) with Bonferroni correction for multiple tests showed that mean peripapillary RNFL thickness was significantly greater for the ARSACS group than all other groups (each $P < 0.0005$). The FRDA group were significantly thinner than all other groups. In addition, the SCA group were significantly thicker than the unaffected controls ($P = 0.001$). The *P*-values are presented in Table 3.

Fundoscopy was performed in 112 patients with other types of genetic ataxia. As expected, a number of typical abnormalities were seen including optic atrophy (in FRDA) and pigmented maculopathy (in SCA7), but none of these patients showed thickened RNFL similar to that seen in ARSACS. Visual acuity was measured in 88 patients (FRDA, $n = 43$; SCA, $n = 34$; others, $n = 11$). No significant differences survived Bonferroni correction for multiple analyses. Performance on Ishihara pseudo-isochromatic plates was assessed in 78 patients (FRDA, $n = 35$; SCA, $n = 34$; others, $n = 9$). There were no significant differences between groups and with ARSACS patients and heterozygotes, although unlike ARSACS patients and heterozygotes, there were patients in all three genetic groups who could not identify more than half of the plates.

Patients with ataxia of unknown cause

Forty-five patients were assessed, for whom no clear genetic or metabolic cause of ataxia including ARSACS had been identified, and none was a heterozygote for a *SACS* gene mutation. All patients except two had average peripapillary RNFL thickness below 110 µm with the lowest value being 45.5 µm. Twenty-two patients also had both Snellen visual acuity and Ishihara colour plates assessed. There were no significant differences in visual acuity or colour vision between the cases of unknown cause and any other group, although again, unlike the patients with ARSACS and *SACS* gene mutation heterozygotes, the group of cases of unknown cause included individuals with extremely poor vision.

One patient showed average peripapillary RNFL thickness slightly above the lowest value for an ARSACS patient (119.3 µm). There was no other ocular explanation for this slightly increased level of RNFL thickening (124.0 µm). There were no point mutations in the *SACS* gene by the Illumina TruSeq Custom Amplicon technique described above. There was also no evidence of deletion or multiplication of *SACS* gene exons by multiplex ligation-dependent probe amplification (MLPA; Dr Filippo Santorelli, personal communication). In addition, the case showed no mutations in a panel of genes known to cause spastic ataxia (Supplementary Table 1) and was negative for SCA1–3, 6 and 7, FRDA, BSCL2, connexion-32, SPG7 and mitochondrial point mutations.

Table 3 ***P*-values for ANCOVA corrected for age with Bonferroni correction**

	SACS Hetero-zygotes	FRDA	SCAs	Other genetic ataxias	Ataxia of unknown cause	Controls
ARSACS	<0.0005*	<0.0005*	<0.0005*	<0.0005*	<0.0005*	<0.0005*
SACS Heterozygotes		<0.0005*	0.692	1.0	1.0	1.0
FRDA			0.001*	0.001*	<0.0005*	<0.0005*
SCAs				1.0	0.107	0.001*
Other genetic ataxias					1.0	1.0
Ataxia of unknown cause						1.0

*Significant at <0.05.

Discussion

To our knowledge, this is the largest cohort of patients with ARSACS and other genetic ataxias to undergo systematic evaluation by OCT and comprehensive visual assessment. This study shows that OCT is a helpful tool in distinguishing ARSACS from other genetically diagnosed causes of progressive ataxia as well as cases of unknown cause and can therefore help to guide genetic testing. In our study, an average peripapillary RNFL thickness of 119 μm on TD-OCT showed the greatest differentiation between ARSACS and other causes of ataxia. Amongst patients with symptomatic ataxia (i.e. ARSACS versus all other causes of ataxia), this gave a sensitivity of 100% and a specificity of 99.4% (area under ROC curve 1.000, $P < 0.001$), and a positive predictive value of 94.4%, a negative predictive value of 100%, a false positive rate of 0.6% and a false negative rate of 0%.

One case of ataxia of unknown cause had average peripapillary RNFL thickness just above this threshold (124.0 μm). Spectral domain-OCT (SD-OCT) confirmed global RNFL thickening; however, the foveal architecture was normal in contrast to patients with genetically proven ARSACS where ganglion cells and their axons may be seen to extend across the fovea. This additional feature of the OCT evaluation may represent a means of distinguishing borderline cases.

In addition, patients should first be thoroughly assessed to exclude acute causes of RNFL thickening such as Leber's hereditary optic neuropathy and optic neuritis. Fundoscopy should always be performed to exclude papilloedema and retinitis pigmentosa as other causes of thickened RNFL. Typically, ARSACS patients also do not have accompanying visual symptoms, other than those associated with cerebellar eye signs such as nystagmus. Thus, their presence should alert the clinician to an alternative diagnosis or an additional unrelated cause of ocular pathology. Similarly, patients diagnosed with ARSACS undergoing assessment in the neurology or ophthalmology clinics can be reassured that visual loss is rare in ARSACS and unrelated to RNFL thickening.

In a previous publication from our group we reported mild thickening of the RNFL in two unaffected heterozygous carriers of *SACS* gene mutations (Nethisinghe *et al.*, 2011). However, the average RNFL thickness in both these cases was 115.5 μm, which falls below the threshold found in this study (119 μm) to distinguish ARSACS from non-ARSACS patients. Moreover, in the present study we have examined a further 13 heterozygous carriers of *SACS* gene mutations and in all cases the RNFL thickness was below 119 μm.

There was an inverse correlation between average peripapillary RNFL thickness and both age at examination and age at onset. However, there was only a trend towards, but not a statistically significant, positive correlation between average peripapillary RNFL thickness and disease duration. Peripapillary RNFL thickness is known to decrease very slowly by 0.18 to 0.32 μm/year in unaffected individuals (Girkin *et al.*, 2011; Kim *et al.*, 2011) due to decline in retinal ganglion cell axon numbers with age. This process is so slow in unaffected individuals that it is unlikely to interfere with the results in this study. The natural history of RNFL thickening in ARSACS patients is unknown. Whilst cross-sectional studies such as this provide some data relating to effects of age on RNFL thickness, longitudinal studies of RNFL thickness in ARSACS are required to answer this question definitively and may provide the identification of a novel biomarker.

The underlying nature of the retinal changes seen in ARSACS remains unknown. Clinically, the thickened retinal nerve fibres appear as radial white or yellow streaks emanating from the optic disc, most commonly in the papillomacular region, and sometimes obscure the retinal vessels (Fig. 1A). These have been described as 'myelinated retinal fibers' (Bouchard, 1991) or 'retinal hypermyelination' (Gücüyener *et al.*, 2001; Ogawa *et al.*, 2004; Takiyama, 2006; Prodi *et al.*, 2013). However, to our knowledge there is no pathological or other evidence to support these appellations. Myelin is not normally present in the human retina. Myelination of optic nerve axons occurs by migration of oligodendrocyte progenitors along long axons, starting at the lateral geniculate body and ceasing at the lamina cribrosa of the optic nerve head where they are prevented from penetrating the retina probably by a dense aggregation of astrocytic processes (Fitzgibbon and Nestorovski, 1997; Hunter *et al.*, 1997). The intraretinal course of the retinal ganglion axons is therefore not usually myelinated.

However, myelinated axons are observed in the human retina in ~1% of the population (Straatsma *et al.*, 1981), giving rise to the syndrome of (persistent) myelinated retinal nerve fibres (SMRNF). They usually cause a visual field defect, myopia or amblyopia (Tarabishy *et al.*, 2007). When the eyes of patients with ARSACS are directly compared with those of patients with known myelinated retinal nerve fibres, a number of differences are apparent. In SMRNF, RNFL thickening is only seen where myelinated nerve fibres are visible, whereas in ARSACS RNFL thickening is widespread, including macula thickening, and is present even in subjects without visible RNFL thickening. In SMRNF, the myelinated nerve fibres cause posterior shadowing on OCT obscuring the deeper layers because of hyper-reflectivity, but this feature is not seen in ARSACS. These findings suggest the material deposited in the retina is different in the two cases (Desserre *et al.*, 2011; Vingolo *et al.*, 2011). We suggest the simple and descriptive term 'thickened retinal nerve fibre layer' (Nethisinghe *et al.*, 2011) until their underlying nature is known. A greater understanding of these changes may help elucidate the underlying pathophysiological processes in this condition.

Conclusion

OCT is a cheap, fast and widely available test that is sensitive and specific for identifying characteristic retinal

changes in patients with ARSACS and can help in distinguishing ARSACS from other genetically diagnosed forms of ataxia and cases of unknown cause. We therefore advocate its routine use in the assessment of suspected cases of ARSACS even in the absence of fundoscopic changes. The underlying pathophysiology of these retinal changes remains obscure but there is increasing evidence that the increased thickness is not related to excess myelin.

Acknowledgements

We would like to thank the patients for participating in the study. We would like to thank Dr Arron Cook for assistance in patient recruitment, Dr Maria Vittoria Ercolani and Dr Suman Pili for assistance with OCT scans, Dr Joshua Hersherson for help with the genetic testing, Dr Filippo Santorelli of the IRCCS Fondazione Stella Maris, Calabrone, Italy for performing the *SACS* MLPA analysis and Dr Roy Poh, Neurogenetic Laboratory, National Hospital for Neurology and Neurosurgery, UCLH for his critical review of the manuscript.

Funding

The project received funding from Ataxia UK and the Fondation de l'Ataxie Charlevoix-Saguenay. PG receives funding from the European Commission Framework Project 7 (HEALTH-F2-2010-242193). P.G., M.H.P. and M.M.R. work at University College London Hospitals/University College London, which receives a proportion of funding from the Department of Health's National Institute for Health Research Biomedical Research Centres funding scheme, and receives support from the NIHR Clinical Research Network (CRN). J.P.C. receives funding from the Barts and the London Charity (417/1699).

Supplementary material

Supplementary material is available at *Brain* online.

References

Balestrini S, Clayton LM, Bartmann AP, Chinthapalli K, Novy J, Coppola A, et al. Retinal nerve fibre layer thinning is associated with drug resistance in epilepsy. J Neurol Neurosurg Psychiatry 2016; 87: 396–401.

Barboni P, Savini G, Valentino ML, Montagna P, Cortelli P, De Negri AM, et al. Retinal nerve fiber layer evaluation by optical coherence tomography in Leber's hereditary optic neuropathy. Ophthalmology 2005; 112: 120–6.

Bouchard JP. Recessive spastic ataxia of Charlevoix-Saguenay. Handb Clin Neurol 1991; 16: 451–9.

Bouchard JP, Barbeau A, Bouchard R, Bouchard RW. Autosomal recessive spastic ataxia of Charlevoix-Saguenay. Can J Neurol Sci 1978; 5: 61–9.

Bouchard JP, Richter A, Mathieu J, Brunet D, Hudson TJ, Morgan K, et al. Autosomal recessive spastic ataxia of Charlevoix-Saguenay. Neuromuscul Disord 1998; 8: 474–9.

Clayton LM, Dévilé M, Punte T, Kallis C, de Haan GJ, Sander JW, et al. Retinal nerve fiber layer thickness in vigabatrin-exposed patients. Ann Neurol 2011; 69: 845–54.

Desserre J, Devos D, Sautiere BG, Debruyne P, Santorelli FM, Vuillaume I, et al. Thickening of peripapillar retinal fibers for the diagnosis of autosomal recessive spastic ataxia of Charlevoix-Saguenay. Cerebellum 2011; 10: 758–62.

Engert JC, Berube P, Mercier J, Dore C, Lepage P, Ge B, et al. ARSACS, a spastic ataxia common in Northeastern Quebec, is caused by mutations in a new gene encoding an 11.5-kb ORF. Nat Genet 2000; 24: 120–5.

Fitzgibbon T, Nestorovski Z. Morphological consequences of myelination in the human retina. Exp Eye Res 1997; 65: 809–19.

Fortuna F, Barboni P, Liguori R, Valentino ML, Savini G, Gellera C, et al. Visual system involvement in patients with Friedreich's ataxia. Brain 2009; 132: 116–23.

Garcia-Martin E, Pablo LE, Gazulla J, Polo V, Ferreras A, Larrosa JM. Retinal nerve fibre layer thickness in ARSACS: myelination or hypertrophy? Br J Ophthal 2013; 97: 238–41.

Gazulla J, Benavente I, Vela AC, Marin MA, Pablo LE, Tessa A, et al. New findings in the ataxia of Charlevoix-Saguenay. J Neurol 2012; 259: 869–78.

Girkin CA, McGwin G, Sinai MJ, Sekhar GC, Fingeret M, Wollstein G, et al. Variation in optic nerve and macular structure with age and race with spectral-domain optical coherence tomography. Ophthalmol 2011; 118: 2403–8.

Grieco GS, Malandrini A, Comanducci G, Leuzzi V, Valoppi M, Tessa A, et al. Novel SACS mutations in autosomal recessive spastic ataxia of Charlevoix-Saguenay type. Neurology 2004; 62: 103–6.

Gücüyener K, Özgül K, Paternotte C, Erdem H, Prud'homme JF, Özgüç M, et al. Autosomal recessive spastic ataxia of Charlevoix-Saguenay in two unrelated Turkish families. Neuropediatrics 2001; 32: 142–6.

Hood DC, Lin CE, Lazow MA, Locke KG, Zhang X, Birch DG. Thickness of receptor and post-receptor retinal layers in patients with retinitis pigmentosa measured with frequency-domain optical coherence tomography. Invest Ophthal Vis Sci 2009; 50: 2328–36.

Hunter SF, Leavitt JA, Rodriguez M. Direct observation of myelination *in vivo* in the mature human central nervous system. A model for the behaviour of oligodendrocyte progenitors and their progeny. Brain 1997; 120: 2071–82.

Jindahra P, Hedges TR, Mendoza-Santiesteban CE, Plant GT. Optical coherence tomography of the retina: applications in neurology. Curr Opin Neurol 2010; 23: 16–23.

Karam EZ, Hedges TR. Optical coherence tomography of the retinal nerve fibre layer in mild papilloedema and pseudopapilloedema. Br J Ophthal 2005; 89: 294–8.

Kim EJ, Hong S, Kim CY, Lee ES, Seong GJ. Attenuated age-related thinning of peripapillary retinal nerve fiber layer in lomg eyes. Kor J Ophthalmol 2011; 25: 248–51.

Klebe S, Depienne C, Gerber S, Challe G, Anheim M, Charles P, et al. Spastic paraplegia gene 7 in patients with spasticity and/or optic neuropathy. Brain 2012; 135: 2980–93.

Manrique RK, Noval S, Aguilar-Amat MJ, Arpa J, Rosa I, Contreras IM. Ophthalmic features of spinocerebellar ataxia type 7. J Neuroophthalmol 2009; 29: 174–9.

Mrissa N, Belal S, Hamida CB, Amouri R, Turki I, Mrissa R, et al. Linkage to chromosome 13q11-12 of an autosomal recessive cerebellar ataxia in a Tunisian family. Neurology 2000; 54: 1408–14.

Nethisinghe S, Clayton L, Vermeer S, Chapple JP, Reilly MM, Bremner F, et al. Retinal imaging in autosomal recessive spastic ataxia of Charlevoix-Saguenay. Neuroophthalmol 2011; 35: 197–201.

Noval S, Contreras I, Sanz-Gallego I, Manrique RK, Arpa J. Ophthalmic features of Friedreich ataxia. Eye 2012; 26: 315–20.

Ogawa T, Takiyama Y, Sakoe K, Mori K, Namekawa M, Shimazaki H, et al. Identification of a SACS gene missense mutation in ARSACS. Neurology 2004; 62: 107–9.

Ouyang Y, Takiyama Y, Sakoe K, Shimazaki H, Ogawa T, Nagano S, et al. Sacsin-related ataxia (ARSACS): expanding the genotype upstream from the gigantic exon. Neurology 2006; 66: 1103–4.

Parkinson MH, Bremner F, Giunti P. Autosomal recessive spastic ataxia of Charlevoix-Saguenay (ARSACS). Adv Clin Neurosci Rehabil 2014; 13: 12–16.

Pablo LE, Garcia-Martin E, Gazulla J, Larrosa JM, Ferreras A, Santorelli FM, et al. Retinal nerve fiber hypertrophy in ataxia of Charlevoix-Saguenay patients. Mol Vis 2011; 17: 1871–6.

Prodi E, Grisoli M, Panzeri M, Minati L, Fattori F, Erbetta A, et al. Supratentorial and pontine MRI abnormalities characterize recessive spastic ataxia of Charlevoix-Saguenay. A comprehensive study of an Italian series. Eur J Neurol 2013; 20: 138–46.

Pula JH, Towle BL, Staszak VM, Cao D, Bernard JT, Gomez CM. Retinal nerve fibre layer and macular thinning in spinocerebellar ataxia and cerebellar multisystem atrophy. Neuroophthalmol 2011; 35: 108–14.

Savini G, Bellusci C, Carbonelli M, Zanini M, Carelli V, Sadun AA, et al. Detection and quantification of retinal nerve fiber layer thickness in optic disc edema using stratus oct. Arch Ophthal 2006; 124: 1111–17.

Seyer LA, Galetta K, Wilson J, Sakai R, Perlman S, Mathews K, et al. Analysis of the visual system in Friedreich ataxia. J Neurol 2013; 260: 2362–9.

Stevens JC, Murphy SM, Davagnanam I, Phadke R, Anderson G, Nethisinghe S, et al. The ARSACS phenotype can include supranuclear gaze palsy and skin lipofuscin deposits. J Neurol Neurosurg Psychiatry 2013; 84: 114–16.

Straatsma BR, Foos RY, Heckenlively JR, Taylor GN. Myelinated retinal nerve fibers. Am J Ophthal 1981; 91: 25–38.

Takiyama Y. Autosomal recessive spastic ataxia of Charlevoix-Saguenay. Neuropathology 2006; 26: 368–75.

Tarabishy AB, Alexandrou TJ, Traboulsi EI. Syndrome of myelinated retinal nerve fibers, myopia, and amblyopia: a review. Survey Ophthal 2007; 52: 588–96.

Thiffault I, Dicaire MJ, Tetreault M, Huang KN, Demers-Lamarche J, Bernard G, et al. Diversity of ARSACS mutations in French-Canadians. Can J Neurol Sci 2013; 40: 61–6.

Van Lint M, Hoornaert K, Ten Tusscher MPM. Retinal nerve fiber layer thickening in ARSACS carriers. J Neurol Sci 2016; 370: 119–22.

Vermeer S. Clinical and genetic characterisation of autosomal recessive cerebellar ataxias. PhD Thesis. Radboud University, Nijmegen, Netherlands, 2012.

Vermeer S, Meijer RP, Pijl BJ, Timmermans J, Cruysberg JR, Bos MM, et al. ARSACS in the Dutch population: a frequent cause of early-onset cerebellar ataxia. Neurogenetics 2008; 9: 207–14.

Vingolo EM, Di Fabio R, Salvatore S, Grieco G, Bertini E, Leuzzi V, et al. Myelinated retinal fibers in autosomal recessive spastic ataxia of Charlevoix-Saguenay. Eur J Neurol 2011; 18: 1187–90.

Yu-Wai-Man P, Pyle A, Griffin H, Santibanez-Korev M, Horvath R, Chinnery PF. Abnormal retinal thickening is a common feature among patients with ARSACS-related phenotypes. Br J Ophthal 2014; 98: 711–13.